

How accurately can we measure the W cross section?

S. Frixione

INFN, Sezione di Genova, Italy
E-mail: Stefano.Frixione@cern.ch

M.L. Mangano

CERN, Theoretical Physics Division, Geneva, Switzerland
E-mail: Michelangelo.Mangano@cern.ch

ABSTRACT: We study the QCD sources of systematic uncertainties in the experimental extraction of the W cross section at hadron colliders. The uncertainties appear in the evaluation of the detector acceptances used to convert the number of observed events into a total production cross section. We consider the effect of NLO corrections, as well as of the inclusion of parton showers, and evaluate the impact of spin correlations and of PDF and scale uncertainties.

Contents

1. Introduction	1
2. Preliminaries	3
3. Results: shower effects at LO and NLO	4
4. Results: PDF and scale uncertainties	10
5. Conclusions	14

1. Introduction

W production, through its leptonic decays, features one of the cleanest signatures at hadronic colliders, with a high- p_T charged lepton recoiling against missing energy [1]–[4]. This distinctive signature and the large production rates allow the measurements of the W mass (m_W) performed at the Tevatron [5]–[7] to be competitive with LEP2 results; a further improvement is expected at the LHC. Accurate measurements of the total W width (Γ_W) will also be obtained. The experimental techniques necessary to perform these measurements are well known [8, 9], and tested extensively at the Tevatron Run I: Γ_W has been extracted with “indirect” methods [10, 11] (in which the measured quantity is the ratio of the Z over the W cross section), and with “direct” methods [12, 13] (in which the measured quantity is the distribution of the W transverse mass). In both cases, a firm control is mandatory on the theoretical predictions for the $p\bar{p} \rightarrow W + X$ or $pp \rightarrow W + X$ production processes; the cross sections for these can be schematically written as follows:

$$\sigma^{\text{th}}(W) = \sum_{ab} \mathcal{P}_{ab} \otimes \hat{\sigma}_{ab}(W). \quad (1.1)$$

Here, \mathcal{P}_{ab} is the product of the parton density functions (PDFs) of the partons a and b (quarks and gluons) in the colliding protons/antiprotons. The PDFs cannot be computed in QCD at present, and are extracted from global fit to data (dominated by DIS); on the other hand the quantity $\hat{\sigma}_{ab}(W)$, the cross section of the process $ab \rightarrow W + X$, is theoretically computable. In fact, the overwhelming majority of the theoretical work on W production has the scope of improving the accuracy with which $\hat{\sigma}_{ab}(W)$ is known. NLO QCD corrections have been computed a long time ago [14]–[18], in a series of papers which pioneered the factorization techniques in perturbation theory. Total rates to NNLO accuracy have been presented in ref. [19]–[20]; recently, the NNLO result for the rapidity of the W has also become available [21], the first differential distribution ever to be computed at this order in α_s . The resummation of the leading and next-to-leading logarithms

of p_T^W/m_W , relevant to the small- p_T^W region where the previously mentioned fixed-order results are unreliable, has been incorporated in a code available to experiments [22]. EW corrections to the W cross section have been shown to be non negligible [23]–[25], with effects up to 5%; fortunately, the dominant contribution there is due to photon emission, which can be implemented in Monte Carlos with multiple QED radiation [26], or combined with resummed QCD formulae [27] (which is especially relevant to m_W measurements).

The measurements of the W mass or width are performed by solving for m_W or Γ_W the following equation

$$\sigma^{\text{th}}(W) = \sigma^{\text{exp}}(W), \quad (1.2)$$

where $\sigma^{\text{exp}}(W)$ is the experimental result for the relevant observable. This can be written as follows:

$$\sigma^{\text{exp}}(W) = \frac{1}{\text{BR}(W \rightarrow l\nu)} \frac{1}{\int \mathcal{L} dt} \frac{N^{\text{obs}}}{A_W}, \quad (1.3)$$

where $\text{BR}(W \rightarrow l\nu)$ is the branching ratio for the leptonic decay of the W considered, $\int \mathcal{L} dt$ is the integrated hadron luminosity, N^{obs} is the number of detected signal events, and A_W is the acceptance, namely the fraction of events which pass the selection cuts of the experimental analysis¹. A procedure alternative to that of measuring the W mass or width is that of using the world averages for m_W and Γ_W , and to solve eq. (1.2) for $\int \mathcal{L} dt$; in this way, W production is treated as a (hadron) *luminosity monitor*. The use of hard processes as luminosity monitors is a very interesting possibility in the high-energy regime of the LHC, as opposed to the more traditional determination of the luminosity through the knowledge of the total hadronic cross section; a necessary condition for this to happen is that the hard cross section must be reliably computed with small uncertainty. The procedure can be pushed a step further, and eq. (1.2) can be solved for $\mathcal{P}_{ab} \int \mathcal{L} dt$, or for \mathcal{P}_{ab} ; thus, W production is used in the former case as a *parton* luminosity monitor, and in the latter case to determine the PDFs. In both cases, the difficulty lies in the sum over the parton labels appearing in eq. (1.1): one needs to devise a way to force the particular combination of partons he is interested in to be the dominant one in that sum. This always implies the necessity of considering differential W distributions. A well known example is the determination of the ratio of the d and u parton densities, which is accessible through the rapidity distribution of the W . More details on the use of W production as a luminosity monitor or in the context of PDF determination can be found in refs. [28, 29, 30].

Equation (1.2) only involves W cross sections. However, the W 's are not detected as such by experiments, but only through charged leptons and missing energy; furthermore, this detection necessarily takes place only in a part of the final-state phase space, either because of limited detector acceptance, or to avoid regions where the backgrounds are so large that the determination of the signal is totally unreliable. Thus, the quantity N^{obs} that appears in eq. (1.3) is obtained after applying detector- and analysis-dependent (lepton) cuts on a very complex final state. The rescaling of N^{obs} by $1/A_W$ allows one to relate this quantity to the relevant W cross section; in other words, acceptance corrections provide an

¹We neglect for simplicity the discussion of the experimental *efficiency* with which events within the acceptance can be detected.

estimate of the number of undetected events. The acceptances need therefore be computed with a program that is able to reliably describe in full details the final state emerging from W production, which typically means an event generator. The following issues then arise: how accurately can these acceptance corrections be calculated? Does the accuracy of the acceptance calculation match the intrinsic accuracy of the theoretical prediction for the W cross section? Generally speaking, the answer to the latter question is negative: the very high accuracy of the theoretical computations of the W cross section is due to the fact that these computations are fully inclusive, which is not the case for the codes used to obtain the acceptances. However, if acceptance cuts only involve the leptons coming from the W decay, then one may use one of the fixed-order computations [14]–[21], letting the W decay isotropically in its rest frame to get the final-state leptons. This procedure may lead to large errors: although the W distributions are correctly predicted by these computations, the lepton distributions are not, since the spin correlations are neglected between the leptons and the initial-state partons. NLO results are available [31] that include such spin correlations, but analogous NNLO results are beyond current capabilities. It should be stressed that the computations that include EW corrections [24, 25] do include lepton spin correlations.

The aim of this paper is that of assessing the accuracy to which acceptances for W signals can be estimated at the Tevatron and the LHC. We shall limit ourselves to considering the QCD effects that may change the computation of the acceptances as obtained with standard parton shower Monte Carlos.

The paper is organized as follows: in sect. 2 we introduce our conventions and notations; sects. 3 and 4 present the results for acceptances and distributions, and in sect. 5 we give our conclusions.

2. Preliminaries

We focus on W production at the Tevatron $p\bar{p}$ collider ($\sqrt{S} = 1.96$ TeV) and at the LHC (pp , $\sqrt{S} = 14$ TeV), and assume in all cases leptonic decays of the W (for the sake of definiteness, we shall consider $W \rightarrow e\nu$; lepton mass effects will be neglected throughout this paper). In each case, we shall discuss two possible sets of experimental cuts, selected to reflect realistic detector capabilities, and to better illustrate how different physics effects have different impacts on the acceptances depending on the event definition.

For the Tevatron, we define the following cuts:

- **Cut 1 :** $p_T^e > 20 \text{ GeV} , \quad |\eta^e| < 1 , \quad \cancel{E}_T > 20 \text{ GeV} ; \quad (2.1)$

- **Cut 2 :** $p_T^e > 20 \text{ GeV} , \quad 1 < |\eta^e| < 2.5 , \quad \cancel{E}_T > 20 \text{ GeV} . \quad (2.2)$

In both cases, we identify \cancel{E}_T with the transverse momentum of the neutrino; p_T^e and η^e are the transverse momentum and the rapidity of the electron. The different rapidity ranges for the two cases mimic typical selection cuts used by the Tevatron experiments, and provide a useful separation between regions of the W rapidity spectrum which have different sensitivities to some of the sources of uncertainty, such as the PDFs. At the LHC

we define instead:

- **Cut 1 :** $p_T^e > 20 \text{ GeV} , \quad |\eta^e| < 2.5 , \quad \cancel{E}_T > 20 \text{ GeV} ; \quad (2.3)$

- **Cut 2 :** $p_T^e > 40 \text{ GeV} , \quad |\eta^e| < 2.5 , \quad \cancel{E}_T > 20 \text{ GeV} . \quad (2.4)$

In this case the selection with higher p_T^e threshold is mostly intended to provide an example of a cut which is very sensitive to the accuracy of the theoretical computation. In addition, large values of p_T^e will be used in the LHC triggers, to cope with the huge inclusive-electron signal and background rates.

We now define our theoretical calculations in more detail:

- LO: parton-level LO QCD;
- LO+HERWIG: parton-level LO QCD, evolved through the HERWIG shower [32]. No matrix-element corrections to the parton shower [33]–[35] have been included, to preserve the LO nature of this step;
- NLO: parton-level NLO QCD;
- MC@NLO: parton-level NLO QCD, merged with the HERWIG parton shower as discussed in refs. [36, 37]. Version 2.31 of MC@NLO is used.

The LO parton-level computations have been performed with ALPGEN [38]. The NLO matrix elements of ref. [31] have been implemented in a fully-differential code according to the formalism of refs. [39, 40]; by turning off the $\mathcal{O}(\alpha_s)$ corrections, complete agreement has been found with the results obtained with ALPGEN for all the W and lepton observables considered. All of the cases above include the spin correlations between the decay leptons and the partons entering the hard matrix elements. For our comparisons, we shall also consider the case in which spin correlations are turned off, an option implemented by simply letting the W boson decay with a pure phase-space distribution. All W -width effects are included, and we generate events for which the dilepton pair has a mass within the range $m_W - 30\Gamma_W < m_{e\nu} < m_W + 30\Gamma_W$. The production rate outside this range is below 10^{-3} of the total.

Our input parameters are defined by tree-level electroweak gauge invariance [38] with fixed input values for m_W , m_Z and G_F :

$$m_W = 80.419 \text{ GeV} , \quad \Gamma_W = 2.048 \text{ GeV} , \quad \sin^2 \theta_W = 0.222 . \quad (2.5)$$

As a default PDF set for all the calculations we use the NLO set MRST2001 [41], with $\alpha_s(M_Z) = 0.119$. The default scale choice is $\mu_R = \mu_F = \mu_0 \equiv \sqrt{m_W^2 + p_T^{W^2}}$.

3. Results: shower effects at LO and NLO

In this section we compute acceptances and total and differential cross sections, comparing the results of the four theoretical approaches defined in the previous section. We shall emphasize in particular the role of NLO corrections, and that of the shower acting on

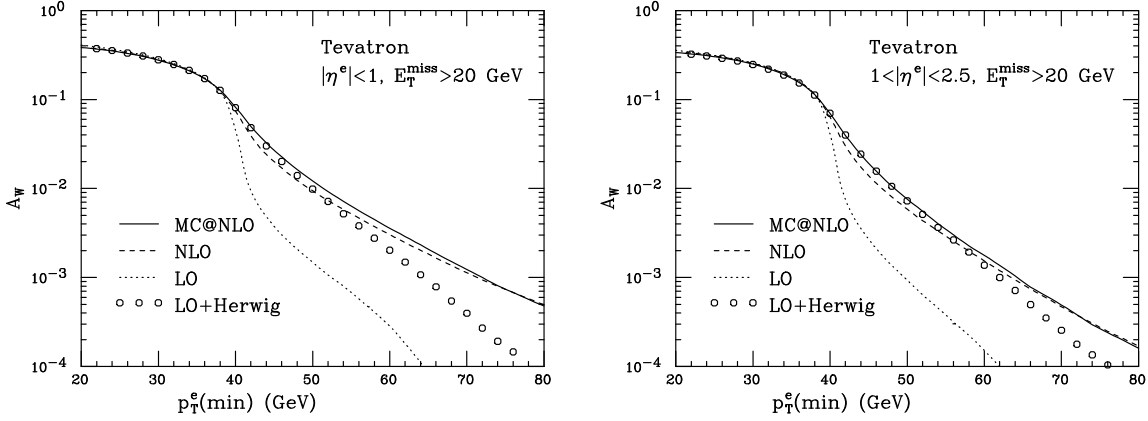


Figure 1: Acceptances as a function of the minimum electron transverse momentum, for the two sets of cuts considered at the Tevatron.

top of the LO and NLO parton-level matrix elements. The effects of neglecting the spin correlations for the W decay products will also be considered here.

We start with the lepton transverse momentum spectra, shown in fig. 1 and 2 for the Tevatron and the LHC, respectively. The spectra are plotted in the form of acceptances as a function of the minimum electron transverse momentum ($p_T^e(\text{min})$), in events which satisfy the η^e and \cancel{E}_T cuts:

$$A_W(p_T^e(\text{min})) = \frac{1}{\sigma^{(tot)}} \int_{p_T^e(\text{min})}^{\sqrt{S}/2} dp_T^e \frac{d\sigma}{dp_T^e}(\text{cuts}), \quad (3.1)$$

where $\sigma^{(tot)}$ is the total W production cross section, evaluated case by case in the appropriate scheme (LO or NLO). Since at the LHC both cut 1 and cut 2 require the same constraints on η^e and \cancel{E}_T , there is only one plot in this case. The four curves in each plot correspond to the four theoretical computations introduced before.

There are clear differences among the four calculations in the high- p_T^e region. The large difference between the LO and the other results is due to the fact that the LO is the only case in which $p_T^W = 0$, which implies that $p_T^e \leq m_W/2$; thus, at the LO the high- p_T^e region is only populated by those events contributing to the tail of the W mass spectrum. The addition of the parton shower improves the situation, since the W acquires a transverse momentum by recoiling against the partons emitted by the shower. However, it is well known that the p_T^W distribution which originates in this way is considerably softer than that predicted at the NLO, since the shower lacks the hard $\mathcal{O}(\alpha_s)$ effects included in the NLO matrix elements. This fact is reflected in the large differences at $p_T^e \sim m_W$ between the LO+HERWIG and the NLO/MC@NLO predictions. Notice finally that while the NLO and MC@NLO results match quite well in the regions $p_T^e \lesssim m_W/2$ and $p_T^e \gtrsim m_W$, the MC@NLO acceptance is larger than the NLO one when $m_W/2 \lesssim p_T^e \lesssim m_W$. While the high- p_T region is not relevant to the determination of the total cross section (since trigger

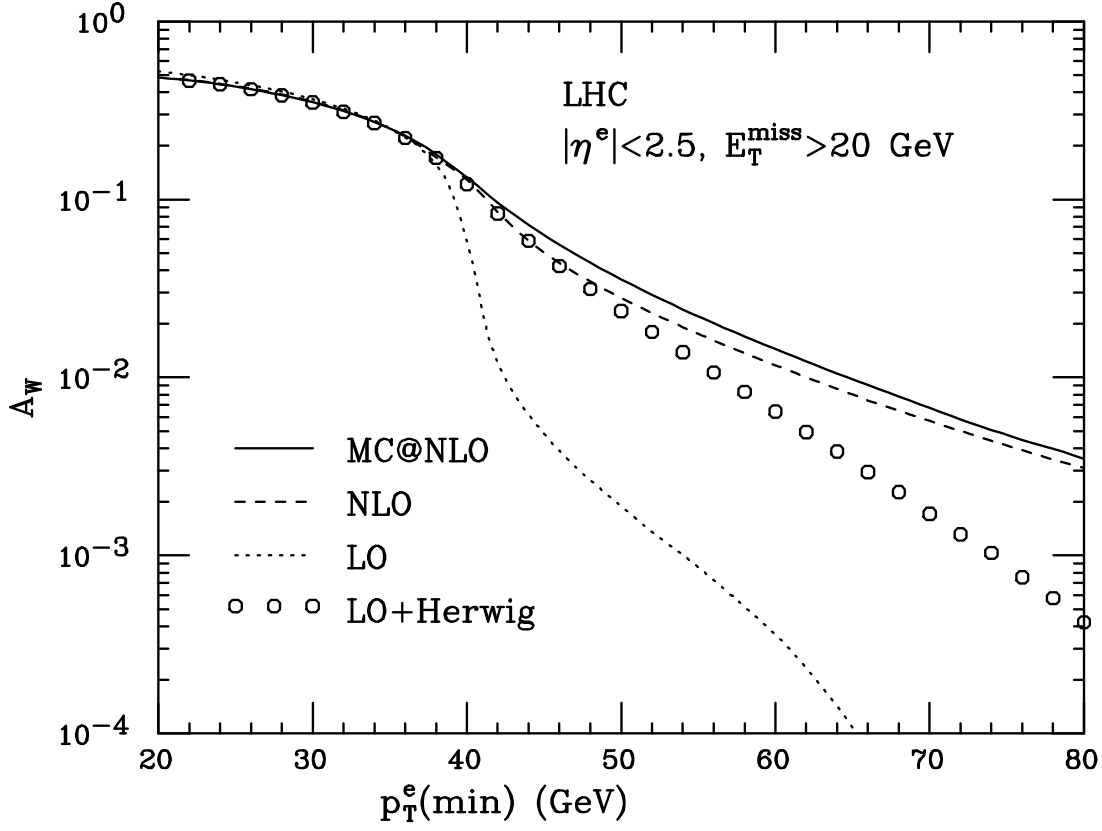


Figure 2: Acceptances as a function of the minimum electron transverse momentum, at the LHC.

thresholds are typically below the $m_W/2$ value), it may play a role in the determination of the W width, which is extracted from the shape of the high-transverse-mass spectrum of the $\ell\nu$ pair [12, 13].

The differences between the various approaches are much smaller in the small- p_T^e region. In fig. 3 we plot the acceptance defined as follows:

$$A_W(\eta^e(\max)) = \frac{1}{\sigma^{(tot)}} \int_0^{\eta^e(\max)} d|\eta^e| \frac{d\sigma}{d|\eta^e|}(\text{cuts}), \quad (3.2)$$

as a function of the maximum electron rapidity ($\eta^e(\max)$), in events which satisfy the $p_T^e > 20$ GeV and the \cancel{E}_T cuts; Tevatron (left panel) and LHC (right panel) results are presented. As can be inferred from fig. 3, the relative behaviour of the various results at small p_T^e 's shown in figs. 1 and 2 would not change had we integrated over different ranges in the electron rapidity. This implies that for measurements dominated by small p_T^e 's the uncertainties on the acceptance corrections are basically independent of the electron rapidity range chosen.

In order to allow a closer comparison between the various theoretical approaches, we

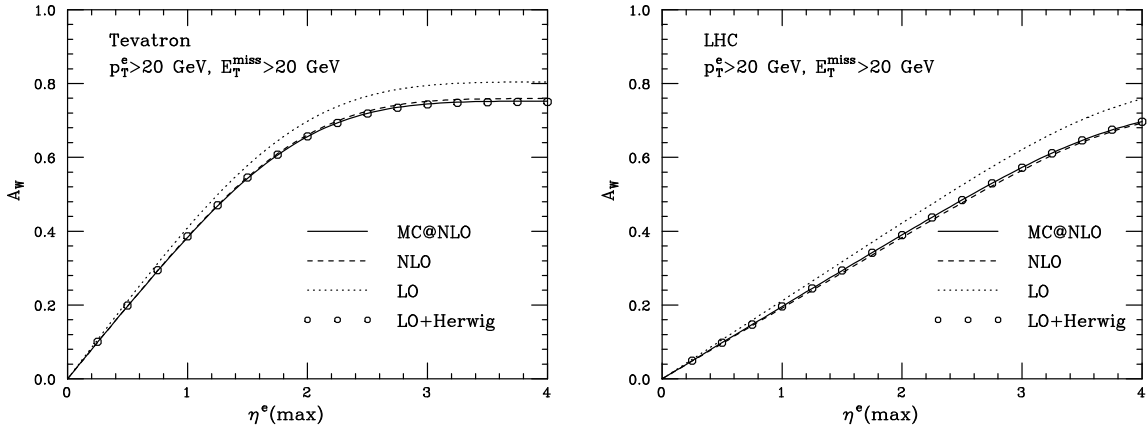


Figure 3: Acceptances as a function of the maximum electron rapidity, at the Tevatron (left panel) and the LHC (right panel), for the smaller p_T^e cut.

present the results² for the rates in tables 1 and 2, and for the acceptances in tables 3 and 4, for the Tevatron and the LHC. In the case of the two sets of cuts considered at the Tevatron, eqs. (2.1) and (2.2), the LO+HERWIG, NLO, and MC@NLO predictions are very close to each other, whereas the LO results differ by more than 5%. It is particularly remarkable that the addition of the shower has a sizable effect on the LO result, while the NLO result remains essentially the same. From the left panel of fig. 3, we see that the LO+HERWIG and the MC@NLO predictions would be even closer to each other, had we considered a larger η^e range than that of cut 1. It is worth noting that, by adding the shower to the LO matrix elements, there are two effects; the first one has already been mentioned, and consists in giving a non-zero p_T to the W . The second effect is due to the fact that, by the backward showering of the partons which enter the LO matrix elements, one may end up with one or two gluons emerging from the colliding hadrons (whereas at the LO only the $q\bar{q}$ combination is possible). This fits nicely into the picture of perturbative QCD corrections; in fact, at the NLO both the $q\bar{q}$ and the $qg + \bar{q}g$ partonic initial states contribute to the results. At the Tevatron the former effect is by far the dominant one, as can be verified by computing the acceptances for cut 1 and 2 at the NLO and considering only the $q\bar{q}$ contributions³, which turn out to be very close to the full NLO results. On the other hand, in the case of cut 1 at the LHC, the $q\bar{q}$ contribution to the NLO acceptance is about 4% larger than the full NLO result. Thus, both effects play a role in the nice agreement between the LO+HERWIG and the MC@NLO results for cut 1 at the LHC, shown in table 4. As already observed in figs. 1 and 2, this situation changes when the p_T^e threshold is increased – see the results relevant to cut 2 in table 4: the MC@NLO prediction is 9% (3%) larger than that of LO+HERWIG (NLO). Here, the difference between MC@NLO and LO+HERWIG is essentially due to the lack of hard emissions in the latter – 40 GeV is large

²The relative errors on our results for total rates are $6 \cdot 10^{-4}$ or smaller, and beyond the last digit reported for acceptances.

³Such contributions are scale and scheme dependent; however, this can be neglected for the sake of the present qualitative argument.

	LO	LO+HW	NLO	MC@NLO
TeV Total	2220	2220	2679	2679
TeV cut 1	907	856	1031	1027
TeV cut 2	790	738	911	900

Table 1: Predictions for the W production rates (in pb) at the Tevatron, with and without the selection cuts defined in eqs. (2.1) and (2.2).

	LO	LO+HW	NLO	MC@NLO
LHC Total	18270	18300	20900	20900
LHC cut 1	9580	8861	9970	10125
LHC cut 2	1060	2230	2699	2776

Table 2: Predictions for the W production rates (in pb) at the LHC, with and without the selection cuts defined in eqs. (2.3) and (2.4).

enough for the collinear approximation built into the shower to start failing. The difference between MC@NLO and NLO has a different origin: in the parton-level LO computation at a fixed m_W , p_T^e cannot assume values larger than $m_W/2$; this implies the possible presence of large logarithmic terms, that arise to all orders beyond the leading one in perturbation theory, and that can be effectively resummed by the shower in MC@NLO. The impact of these logs is less important as one moves away from the threshold, as can be seen from figs. 1 and 2.

The inclusion of NLO matrix elements into a parton shower framework renders the computation of the acceptances by MC@NLO intrinsically more reliable than that performed with a standard Monte Carlo event generator. However, one may wonder whether the accuracy thus obtained is sufficient in the context of an NNLO analysis. From the discussion given above, it seems indeed so. In fact, no qualitatively new kinematic effects appear at the NNLO with respect to the NLO; as far as the computation of the W acceptance is concerned, it is irrelevant whether the W recoils against one or two hard partons (the same would not be true were we interested in the W +jet system). The $p_T^e = m_W/2$ boundary is treated by MC@NLO to all orders, thus including NNLO effects. The partonic initial states that appear for the first time at the NNLO, such as gg , have a very modest impact on W distributions [21], and are anyhow included in MC@NLO through backward showering. Thus, we expect the acceptances computed with MC@NLO to be fairly similar to those that could be computed if we knew how to merge NNLO matrix elements with parton showers.

Given the fact that, as shown before for $p_T^e > 20$ GeV, MC@NLO and NLO give similar

	LO	LO+HW	NLO	MC@NLO
TeV cut 1	0.409	0.386	0.385	0.383
TeV cut 2	0.356	0.333	0.340	0.336

Table 3: Acceptances for the various cuts, at the Tevatron.

	LO	LO+HW	NLO	MC@NLO
LHC cut 1	0.524	0.484	0.477	0.485
LHC cut 2	0.058	0.122	0.129	0.133

Table 4: Acceptances for the various cuts, at the LHC.

results, one may take a different attitude, and use parton-level NNLO results to compute the acceptances. If the cuts chosen do not select *only* the region of small p_T^W (which is not reliably predicted by any fixed-order computation), the result of ref. [21] gives access to the full W kinematics. Unfortunately, no NNLO computation includes lepton spin correlations. These correlations are irrelevant if one is interested in the distributions of the W , but are important if one needs to apply cuts on lepton variables. To document this, we present in table 5 the acceptance results obtained by switching the spin correlations off (namely assuming flat, phase-space decays of the W); we compare the LO, NLO, and MC@NLO results with the analogous ones obtained with full spin correlations, already reported before. Apart from the case of cut 1 at the Tevatron, the effects are very large, with shifts of up to 15%. NLO and MC@NLO are in general close to each other, but no clear pattern emerges when going from LO to NLO; as it should be expected, the LO to NLO ratio depends on the electron rapidity range considered. We thus conclude that, lacking the full information on lepton spin correlations, present NNLO results can only give rough estimates of the acceptances.

We can also consider quantities that are less inclusive than acceptances, such as the rapidity of the W boson (y_W). It has been shown in ref. [21] that the y_W spectrum at NNLO can be very accurately reproduced by rescaling the NLO distribution with the appropriate K factor; interestingly, the rescaled LO distribution is *not* a good approximation of the full NLO distribution. The arguments given before on MC@NLO imply that, by rescaling with the K factor the y_W distribution predicted by MC@NLO, we should get a good approximation of the true NNLO+shower prediction. In fig. 4 we show the fully inclusive y_W spectra for the Tevatron and the LHC. We notice that the inclusion of the shower into both the LO and NLO calculations leads to a slightly more central production, in particular at the LHC. After imposing lepton selection cuts, this effect is reduced at the Tevatron (fig. 5), but remains clearly visible at the LHC at the NLO (fig. 6). In analogy to what done in table 5, we also include the predictions obtained at the LO by switching the spin

	Tevatron			LHC		
	LO	NLO	MC@NLO	LO	NLO	MC@NLO
Cut 1	0.409	0.385	0.383	0.524	0.477	0.485
Cut 1, no spin	0.413	0.394	0.394	0.553	0.510	0.515
Cut 2	0.356	0.340	0.336	0.058	0.129	0.133
Cut 2, no spin	0.389	0.374	0.370	0.075	0.150	0.157

Table 5: Effect of spin correlations on acceptances for the various cuts, at the Tevatron and the LHC.

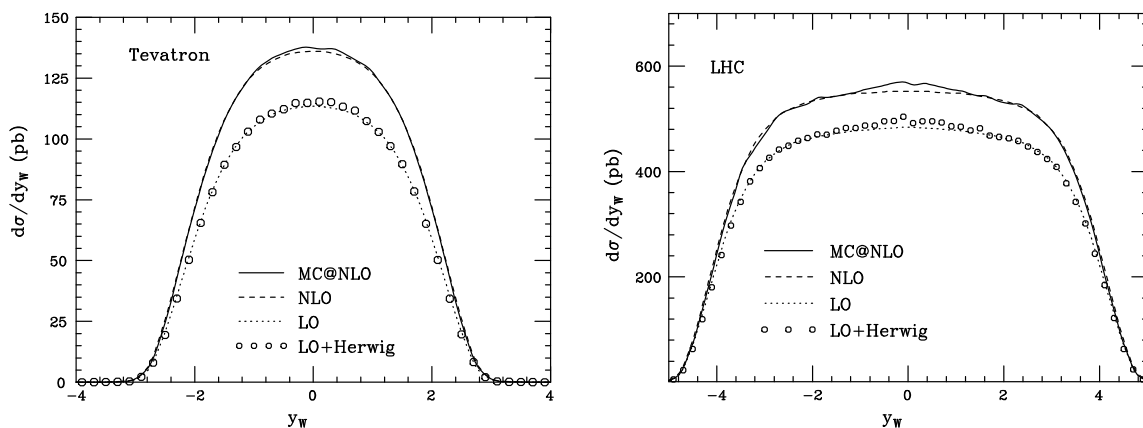


Figure 4: Fully-inclusive W rapidity distribution, at the Tevatron (left panel) and the LHC (right panel).

correlations off (the curves are those labelled “LO, no spin”), which result in significant changes in the shapes of the distributions.

4. Results: PDF and scale uncertainties

In this section we study the sensitivity of the acceptances to the uncertainties affecting the PDF sets and to the choices of renormalization/factorization scales.

To assess the PDF uncertainty we have used the 30 MRST2001E sets [42], using the prescription for asymmetric errors proposed in ref. [43] (modified tolerance method). As discussed before, our best estimates of the acceptances are obtained with MC@NLO. Given the results relevant to cuts 1 and 2, we expect the uncertainties relative to the central value to be very similar when computed with MC@NLO or with NLO. Thus, we shall restrict ourselves here to the parton-level NLO computations, which are somewhat faster to perform

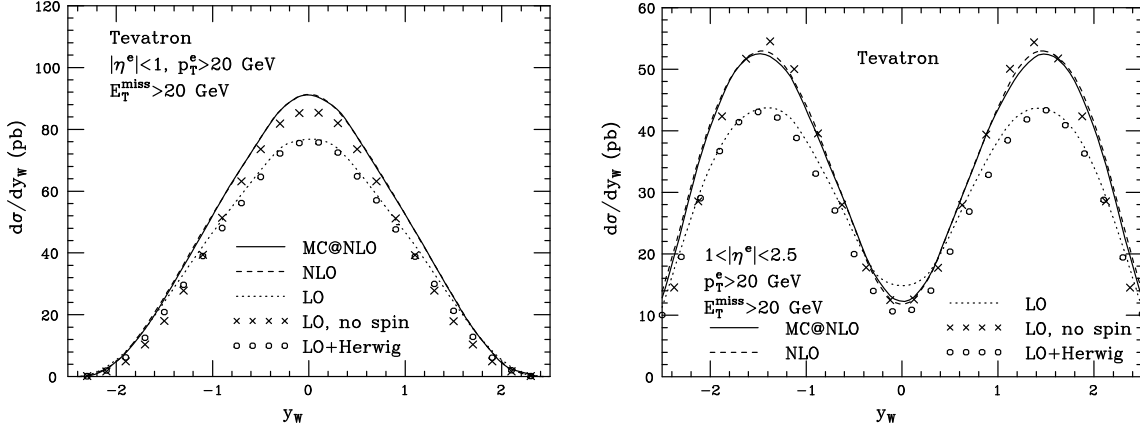


Figure 5: W rapidity distribution at the Tevatron, with lepton cuts.

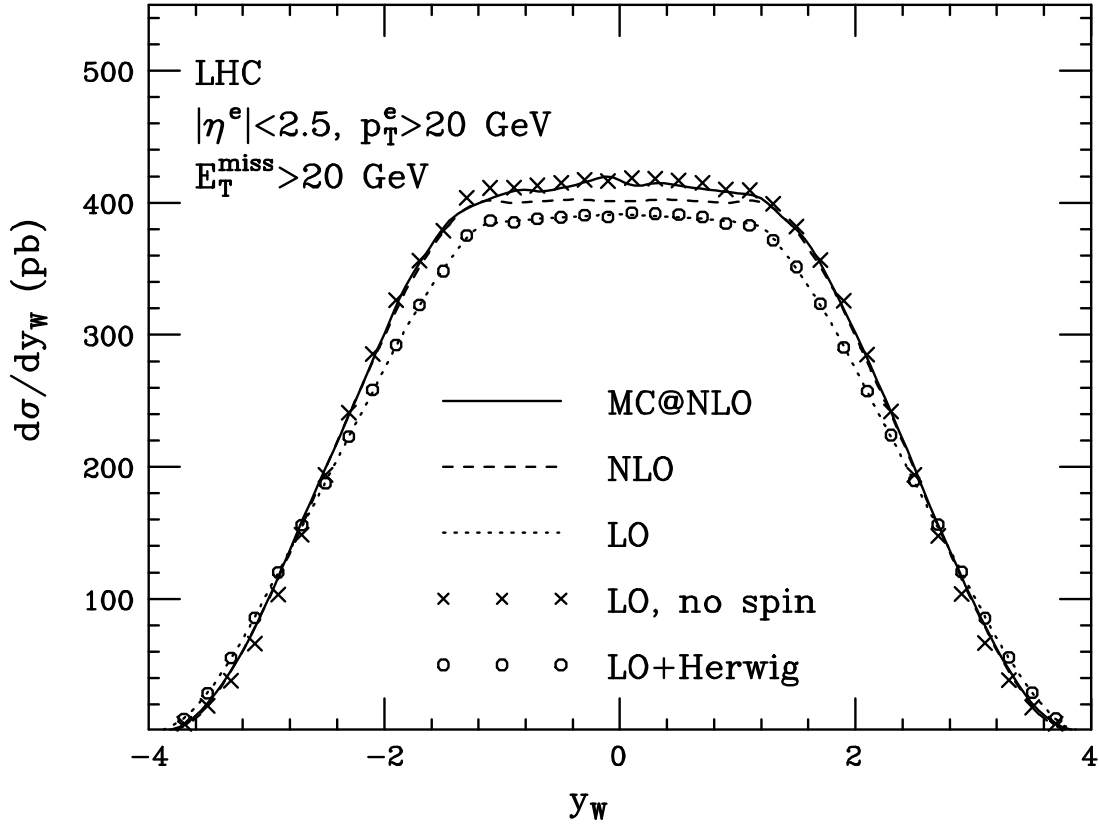


Figure 6: W rapidity distribution at the LHC, with lepton cuts.

than MC@NLO's. Using the default MRST2001E tolerance value of $T = \sqrt{50}$ (see below for further discussions on this point), we obtain the following results for the Tevatron:

$$\sigma(\text{NLO}) = 2679_{-43}^{+26} \text{ pb} \quad (4.1)$$

	$\mu = \mu_0/2$		$\mu = \mu_0$		$\mu = 2\mu_0$	
	NLO	MC@NLO	NLO	MC@NLO	NLO	MC@NLO
TeV cut 1	0.382	0.384	0.385	0.383	0.388	0.385
TeV cut 2	0.339	0.335	0.340	0.336	0.342	0.335

Table 6: Scale dependence of the acceptances, Tevatron.

$$A_W(\text{cut 1}) = 0.3848^{+0.0020}_{-0.0039} \quad (4.2)$$

$$A_W(\text{cut 2}) = 0.3402^{+0.0028}_{-0.0013} \quad (4.3)$$

and for the LHC:

$$\sigma(\text{NLO}) = 20900^{+318}_{-474} \text{ pb} \quad (4.4)$$

$$A_W(\text{cut 1}) = 0.4770^{+0.0048}_{-0.0049} \quad (4.5)$$

$$A_W(\text{cut 2}) = 0.1292^{+0.0007}_{-0.0027} \quad (4.6)$$

To compute the uncertainties shown in these equations, we considered the pulls with respect to the results obtained with the $n = 0$ MRST2001E set. Although the $n = 0$ set is very similar to the default set of MRST2001, the results obtained with the two are not identical for the cross sections (with the $n = 0$ set, we get 2673 pb and 20815 pb at the Tevatron and the LHC respectively) – they are identical for the acceptances; however, these differences being less than 0.5%, we associated the uncertainties computed with the $n = 0$ set with the cross section results relevant to the default set of MRST2001.

We remind the reader that the Hessian method [44], as it has been originally proposed, returns symmetric uncertainties for a given observable. These uncertainties are therefore independent of the central value for the observable considered, at variance with what obtained in eqs. (4.1)–(4.6) with the prescription of ref. [43]. Following ref. [44] we would have obtained

$$\Delta(\sigma(\text{NLO})) = 32 \text{ pb}, \quad \Delta(A_W(\text{cut 1})) = 0.0027, \quad \Delta(A_W(\text{cut 2})) = 0.0018, \quad (4.7)$$

at the Tevatron, and

$$\Delta(\sigma(\text{NLO})) = 386 \text{ pb}, \quad \Delta(A_W(\text{cut 1})) = 0.0047, \quad \Delta(A_W(\text{cut 2})) = 0.0015, \quad (4.8)$$

at the LHC. It is reassuring that these results are in overall agreement with those shown in eqs. (4.1)–(4.6). We notice that both at the Tevatron and the LHC the relative uncertainty on the acceptance is approximately half the size of the uncertainty on the total rate, and at the per cent level. Since the impact of the PDFs on the acceptance is mostly due to the

	$\mu = \mu_0/2$		$\mu = \mu_0$		$\mu = 2\mu_0$	
	NLO	MC@NLO	NLO	MC@NLO	NLO	MC@NLO
LHC cut 1	0.475	0.485	0.477	0.485	0.478	0.484
LHC cut 2	0.130	0.134	0.129	0.133	0.125	0.132

Table 7: Scale dependence of the acceptances, LHC.

η^e cuts, which reflect the y_W distributions, we expect that accurate measurements of the η^e spectra will allow to reduce this uncertainty even further once the data will be available.

We finally point out that the theoretical picture underlying the treatment of PDF uncertainties is far from being established. Although within the Hessian method one formally arrives at the definition of the 1σ error band, in practice the combined effect of the failure of some of the theoretical approximations involved, and of difficulties in the treatment of the correlations between experimental errors, implies the necessity of dropping the rigorous 1σ considerations. At this point, one is forced to introduce an *arbitrariness* in the procedure, parametrized in terms of a single parameter (the tolerance) T , which is the maximum allowed of the $\Delta\chi^2$ variation w.r.t. the parameters of the best PDF fit. The MRST2001E [42] and CTEQ6 [45] sets assume $T = \sqrt{50}$ and $T = 10$ respectively. On this basis alone, and barring the other differences between the parametrizations of refs. [42] and [45], with the latter choice for T the uncertainties of eqs. (4.1)–(4.8) would have been a factor of $\sqrt{2}$ larger. Furthermore, it has been argued that the Lagrange multiplier method [46] may be better suited if one is interested in specific observables, such as the ones considered in this paper. In ref. [42] the PDF uncertainty affecting the W cross section at the LHC, computed according to the Lagrange multiplier method, has been found to be marginally larger than that computed with the Hessian method. We conclude that, although the results of eqs. (4.1)–(4.6) are based on some assumptions that will need further theoretical considerations, they can be considered as reliable estimates, perhaps up to a factor of 1.5, of the PDF uncertainties.

In tables 6 and 7 we finally present the results for the scale dependence of the acceptances at the Tevatron and the LHC. We identify the factorization and renormalization scales, and set them equal to $r_\mu\mu_0$, with $r_\mu = 1/2, 1$ and 2 . The uncertainty at NLO is of the order of 1–2%, depending on the cuts (the largest variation being obtained for cut 2 at the LHC). It is reduced to below 1% with MC@NLO. Although an independent variation of μ_R and μ_F would lead to larger uncertainties, these results suggest a good stability w.r.t. to the addition of NNLO corrections (as shown explicitly in ref. [21] for the case of fully inclusive y_W distributions), and point towards an improved scale dependence of the full NLO+shower result. This behaviour is typical of most of the matched computations, which combine the matrix elements computed to a given order in perturbation theory with the resummation of large logarithmic terms.

5. Conclusions

We summarize here the main conclusions of our study.

- In the case of lepton p_T thresholds at 20 GeV, the addition of the shower corrections to the parton-level LO calculation has a large effect on the acceptances. On the contrary, the addition of the shower changes the NLO parton-level result by only 1%, both at the Tevatron and at the LHC and over the full rapidity range $|\eta^e| < 2.5$. At the LO, the effect of shower corrections increases with the lepton p_T threshold; at the NLO, it first increases (it is about 3% for the 40 GeV threshold at the LHC, and it is larger than 10% around 50 GeV), and then decreases again when the threshold moves towards m_W .
- A major role in the overall acceptance is played by spin correlations. Only their inclusion can guarantee a solid estimate of the acceptance. No clear pattern of evolution of the spin correlations emerges when going from LO to NLO, indicating that no obvious guess can be made on the impact of spin correlations at the NNLO level. As a result, only when spin correlations will be included in the NNLO calculation it will be possible to use this improved result for solid acceptance predictions at the parton level.
- The scale dependence of the acceptance is at a level of 1% or less, suggesting that the NLO approximation is stable relative to the addition of NNLO corrections. This is consistent with the observation of ref. [21] that the shape of the fully inclusive rapidity distribution of the W boson is not altered by NNLO effects. Since the y_W distribution is one of the main elements determining the rapidity acceptance for the final-state charged lepton, it is therefore reasonable to assume that this conclusion survives the presence of analysis cuts.
- Current PDF uncertainties affect the calculation of the acceptance at the level of 1%.

We conclude that the tools currently available (parton-level NLO plus the parton shower, à la MC@NLO) should be sufficient to guarantee an overall theoretical uncertainty on W acceptances due to QCD effects at the level of 2%, with possible improvements coming from an in-situ monitoring of the rapidity distributions, which should reduce the PDF uncertainties. In addition to the QCD effects, the known EW corrections both to the short-distance matrix elements and to the definition of the lepton energy and isolation will need to be included in any solid experimental estimate of the total W cross section. This overall accuracy well matches the best theoretical estimates of the total W cross section, based on NNLO QCD and NLO EW calculations. This opens the way for tests of QCD in hadronic collisions at the per cent level, and for high-precision luminosity monitors based on large-rate and high- p_T observables.

References

- [1] G. Arnison *et al.* [UA1 Collaboration], Phys. Lett. B **122** (1983) 103.

- [2] M. Banner *et al.* [UA2 Collaboration], Phys. Lett. B **122** (1983) 476.
- [3] F. Abe *et al.* [CDF Collaboration], Phys. Rev. Lett. **62** (1989) 1005.
- [4] S. Abachi *et al.* [D0 Collaboration], Phys. Rev. Lett. **75** (1995) 1456 [arXiv:hep-ex/9505013].
- [5] T. Affolder *et al.* [CDF Collaboration], Phys. Rev. D **64** (2001) 052001 [arXiv:hep-ex/0007044].
- [6] V. M. Abazov *et al.* [D0 Collaboration], Phys. Rev. D **66** (2002) 012001 [arXiv:hep-ex/0204014].
- [7] W. Ashmanskas *et al.*, the Tevatron Electroweak Working Group, CDF and D0 Collaborations, arXiv:hep-ex/0311039.
- [8] C. Albajar *et al.* [UA1 Collaboration], Phys. Lett. B **253** (1991) 503.
- [9] J. Alitti *et al.* [UA2 Collaboration], Phys. Lett. B **276** (1992) 365.
- [10] F. Abe *et al.* [CDF Collaboration], Phys. Rev. D **52** (1995) 2624.
- [11] B. Abbott *et al.* [D0 Collaboration], Phys. Rev. D **61** (2000) 072001 [arXiv:hep-ex/9906025].
- [12] T. Affolder *et al.* [CDF Collaboration], Phys. Rev. Lett. **85** (2000) 3347 [arXiv:hep-ex/0004017].
- [13] V. M. Abazov *et al.* [D0 Collaboration], Phys. Rev. D **66** (2002) 032008 [arXiv:hep-ex/0204009].
- [14] G. Altarelli, R. K. Ellis and G. Martinelli, Nucl. Phys. B **157** (1979) 461.
- [15] J. Kubar-Andre and F. E. Paige, Phys. Rev. D **19** (1979) 221.
- [16] K. Harada, T. Kaneko and N. Sakai, Nucl. Phys. B **155** (1979) 169 [Erratum-ibid. B **165** (1980) 545].
- [17] J. Abad and B. Humpert, Phys. Lett. B **80** (1979) 286.
- [18] B. Humpert and W. L. Van Neerven, Phys. Lett. B **85** (1979) 293.
- [19] R. Hamberg, W. L. van Neerven and T. Matsuura, Nucl. Phys. B **359** (1991) 343 [Erratum-ibid. B **644** (2002) 403].
- [20] R. V. Harlander and W. B. Kilgore, Phys. Rev. Lett. **88** (2002) 201801 [arXiv:hep-ph/0201206].
- [21] C. Anastasiou, L. Dixon, K. Melnikov and F. Petriello, arXiv:hep-ph/0312266.
- [22] C. Balazs and C. P. Yuan, Phys. Rev. D **56** (1997) 5558 [arXiv:hep-ph/9704258].
- [23] U. Baur, S. Keller and D. Wackeroth, Phys. Rev. D **59** (1999) 013002 [arXiv:hep-ph/9807417].
- [24] U. Baur, O. Brein, W. Hollik, C. Schappacher and D. Wackeroth, Phys. Rev. D **65** (2002) 033007 [arXiv:hep-ph/0108274].
- [25] S. Dittmaier and M. Kramer, Phys. Rev. D **65** (2002) 073007 [arXiv:hep-ph/0109062].
- [26] C. M. Carloni Calame, S. Jadach, G. Montagna, O. Nicrosini and W. Placzek, Acta Phys. Polon. B **35** (2004) 1643 [arXiv:hep-ph/0402235].
- [27] Q. H. Cao and C. P. Yuan, arXiv:hep-ph/0401026.

- [28] M. Dittmar, F. Pauss and D. Zurcher, Phys. Rev. D **56** (1997) 7284 [arXiv:hep-ex/9705004].
- [29] V. A. Khoze, A. D. Martin, R. Orava and M. G. Ryskin, Eur. Phys. J. C **19** (2001) 313 [arXiv:hep-ph/0010163].
- [30] W. T. Giele and S. A. Keller, arXiv:hep-ph/0104053.
- [31] P. Aurenche and J. Lindfors, Nucl. Phys. B **185**, 274 (1981).
- [32] G. Corcella *et al.*, JHEP **0101** (2001) 010 [arXiv:hep-ph/0011363].
- [33] M. H. Seymour, Comput. Phys. Commun. **90** (1995) 95 [hep-ph/9410414].
- [34] G. Corcella and M. H. Seymour, Nucl. Phys. B **565** (2000) 227 [hep-ph/9908388].
- [35] G. Miu and T. Sjostrand, Phys. Lett. B **449** (1999) 313 [hep-ph/9812455].
- [36] S. Frixione and B. R. Webber, JHEP **0206** (2002) 029 [arXiv:hep-ph/0204244].
- [37] S. Frixione, P. Nason and B. R. Webber, JHEP **0308** (2003) 007 [arXiv:hep-ph/0305252].
- [38] M. L. Mangano, M. Moretti, F. Piccinini, R. Pittau and A. D. Polosa, JHEP **0307** (2003) 001 [arXiv:hep-ph/0206293].
- [39] S. Frixione, Z. Kunszt and A. Signer, Nucl. Phys. B **467** (1996) 399 [arXiv:hep-ph/9512328].
- [40] S. Frixione, Nucl. Phys. B **507** (1997) 295 [arXiv:hep-ph/9706545].
- [41] A. D. Martin, R. G. Roberts, W. J. Stirling and R. S. Thorne, Eur. Phys. J. C **23** (2002) 73 [arXiv:hep-ph/0110215].
- [42] A. D. Martin, R. G. Roberts, W. J. Stirling and R. S. Thorne, Eur. Phys. J. C **28** (2003) 455 [arXiv:hep-ph/0211080].
- [43] Z. Sullivan, Phys. Rev. D **66** (2002) 075011 [arXiv:hep-ph/0207290].
- [44] J. Pumplin *et al.*, Phys. Rev. D **65** (2002) 014013 [arXiv:hep-ph/0101032].
- [45] J. Pumplin, D. R. Stump, J. Huston, H. L. Lai, P. Nadolsky and W. K. Tung, JHEP **0207** (2002) 012 [arXiv:hep-ph/0201195].
- [46] D. Stump *et al.*, Phys. Rev. D **65** (2002) 014012 [arXiv:hep-ph/0101051].